

Supplementary Information to manuscript

"Hysteresis of idealized, instability-prone outlet glaciers under variation of pinning-point buttressing"

Johannes Feldmann¹, Anders Levermann^{1,2,3}, and Ricarda Winkelmann^{1,2}

¹Potsdam Institute for Climate Impact Research (PIK), Potsdam, Germany

²Institute of Physics, University of Potsdam, Potsdam, Germany

³LDEO, Columbia University, New York, USA

Correspondence: Johannes Feldmann (johannes.feldmann@pik-potsdam)

Content

This Supplement contains the following figures:

- **Figure S1:** Temporal evolution of the step-wise forcing (topographic-high elevation) and the associated response in the centerline grounding-line position for the laterally confined simulations.
- 5 – **Figures S2+S3:** Hysteresis curves of the laterally confined simulations for topographic-high locations of $x_{\text{TH}} = 500$ km and $x_{\text{TH}} = 650$ km, respectively (analogous to Fig. 3, where $x_{\text{TH}} = 650$ km).
- **Figure S4:** Hysteresis curves of the laterally unconfined simulations for a topographic-high location of $x_{\text{TH}} = 600$ km (analogous to Fig. 3).
- **Figure S5:** Steady-state centerline profiles for the two laterally unconfined hysteresis experiments (analogous to the
10 profiles from the laterally confined simulations shown in Fig. 2).
- **Figures S6+S7:** Comparison between the different prescribed bed topographies and associated steady-state surface speed fields for the laterally confined simulations versus the laterally unconfined simulations.

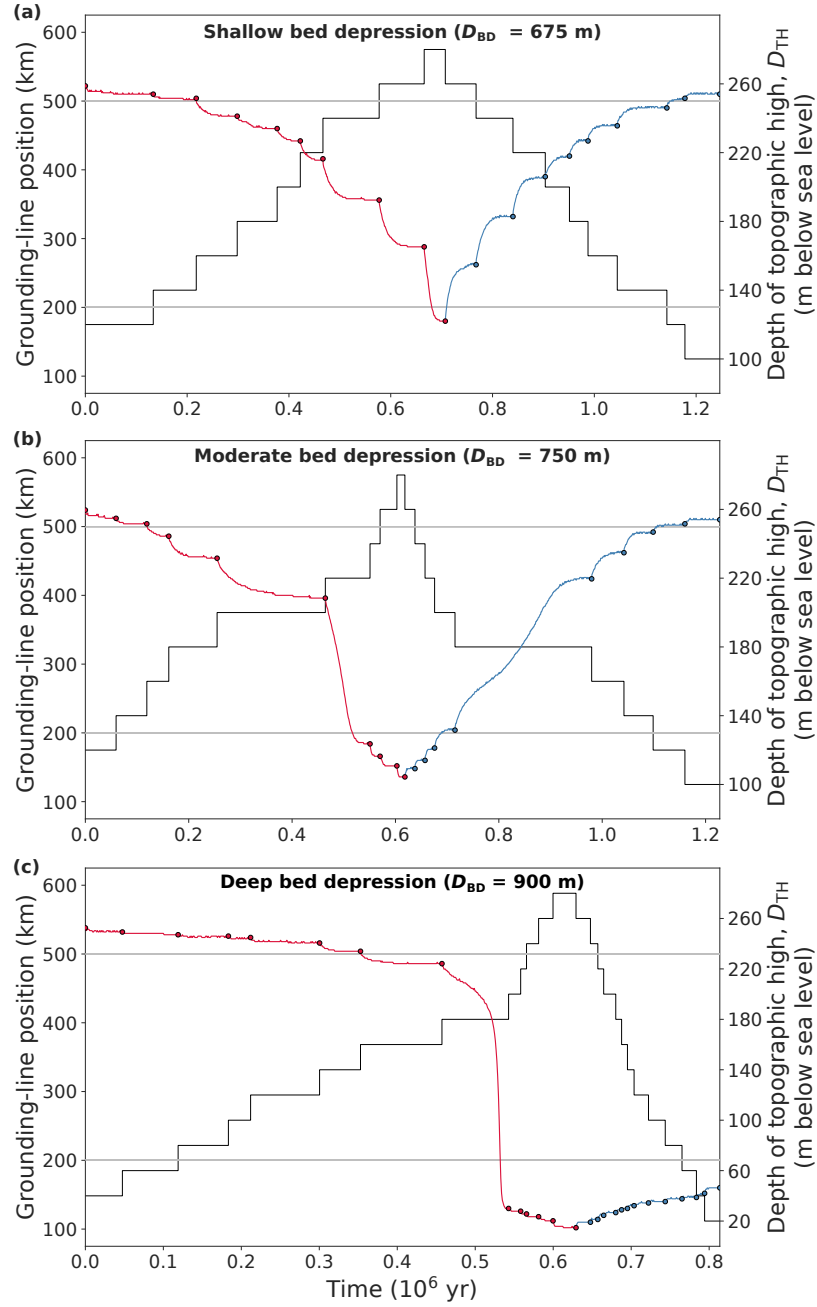


Figure S1. Timeseries of grounding-line evolution in the laterally confined simulations in response to the step-wise increase (red) and subsequent decrease (blue) of the depth of the topographic high (black). The depth of the topographic high is held constant in each individual experiment. The steady-state grounding-line positions at the end of each experiment (used in the corresponding hysteresis curves in Fig. 3) are highlighted by red and blue circles, respectively. The topographic high is located at $x_{TH} = 600$ km. The panels show results for three different bed-depression depths, **(a)** $D_{BD} = 675$ m (shallow), **(b)** $D_{BD} = 750$ m (moderate) and **(c)** $D_{BD} = 900$ m (deep). The two grey horizontal lines mark the range of the retrograde bed section between the tip of the coastal sill (at $x = 500$ km) and the deepest point of the bed depression (at $x = 200$ km).

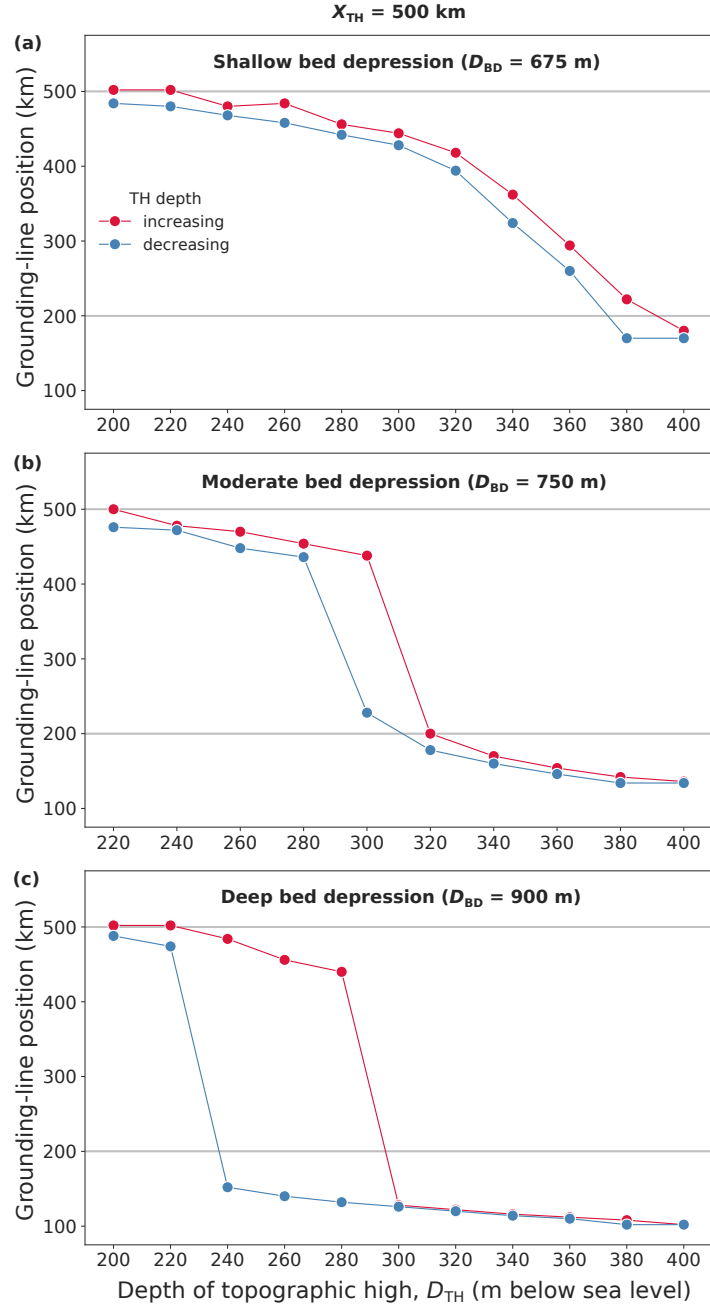


Figure S2. Hysteresis curves of the laterally confined simulations analogous to Fig. 3 for a topographic-high location of $x_{TH} = 500 \text{ km}$.

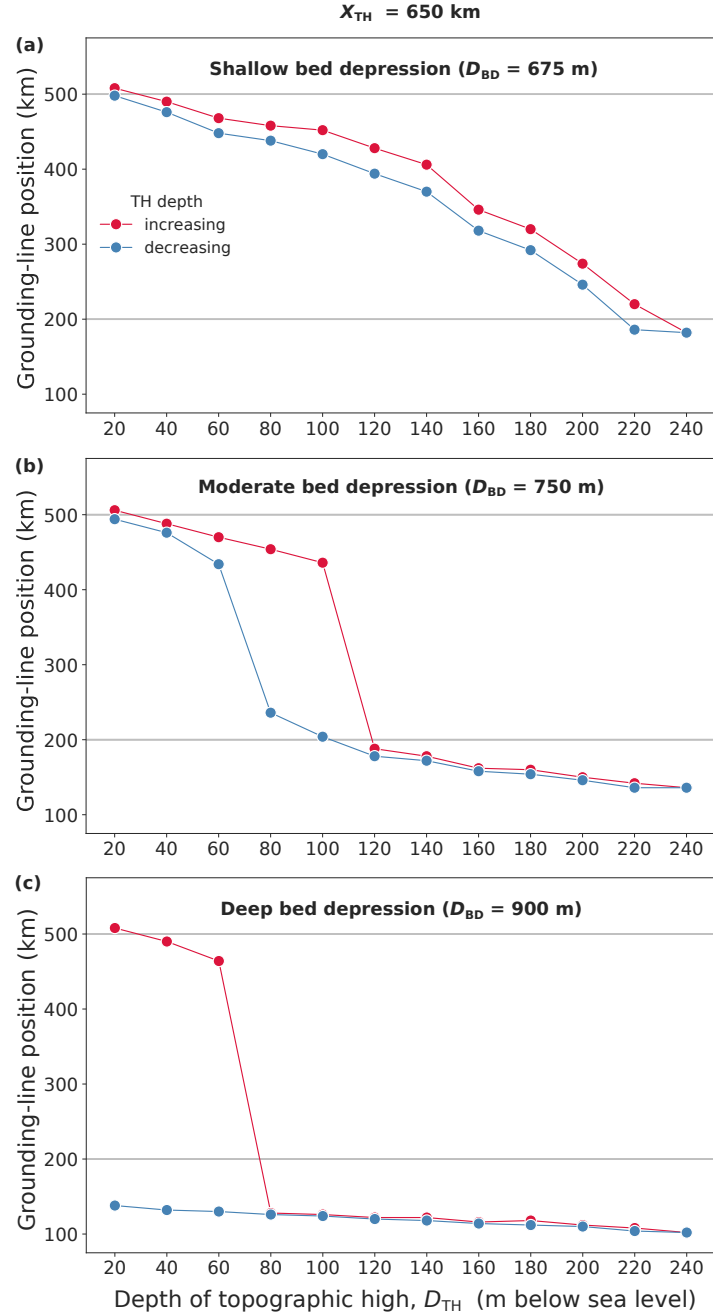


Figure S3. Hysteresis curves of the laterally confined simulations analogous to Fig. 3 for a topographic-high location of $x_{TH} = 650$ km.

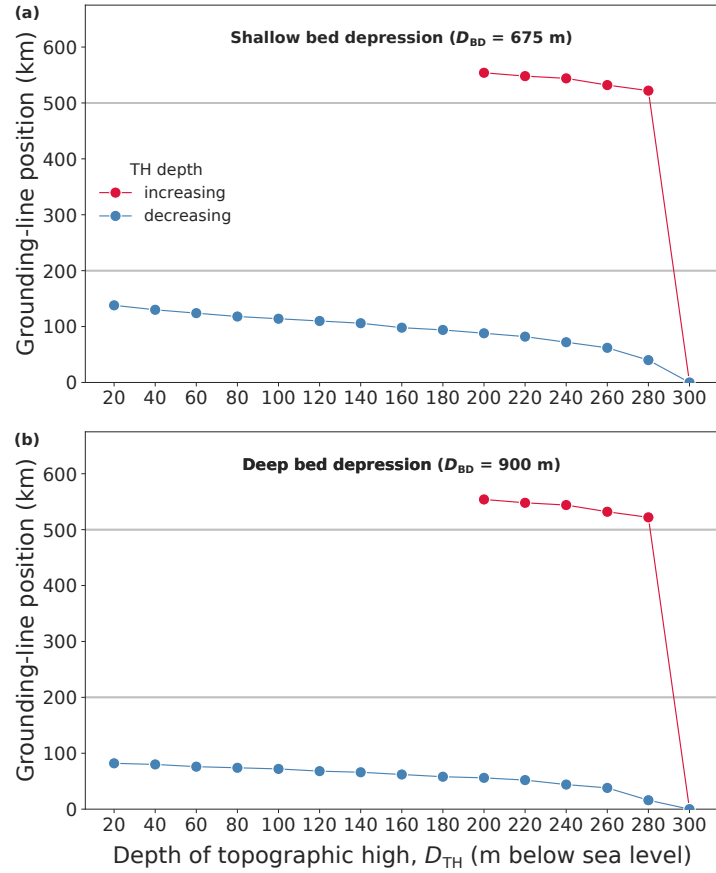


Figure S4. Hysteresis curves of the laterally unconfined simulations, analogous to Fig. 3 (topographic-high location: $x_{TH} = 600$ km).

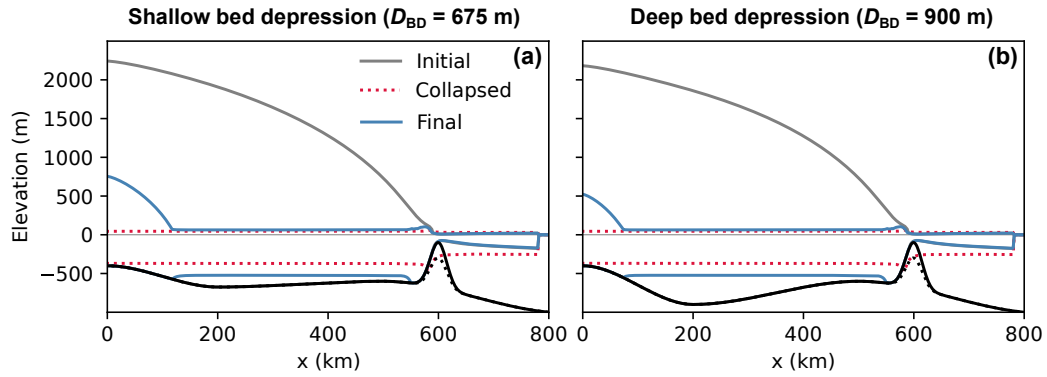


Figure S5. Steady-state centerline profiles for the two laterally unconfined hysteresis experiments, i.e., for **(a)** a shallow bed depression and **(b)** a deep bed depression. The prescribed topographic-high distance is $x_{\text{TH}} = 600$ km. Shown are the initial state before perturbation (grey), the state after the grounded part of the ice-sheet-shelf system has vanished (collapsed, red dotted) and the final state, i.e., after the topographic high has been raised to its original value (blue). Bed topography in black with the dotted profile showing the topographic high at the stage of ice-shelf ungrounding (associated with red dotted profile), i.e., when the topographic high is lowered to a depth of $D_{\text{TH}} = 300$ m. Note that in both cases the collapsed system is an ice shelf that is still grounded on the topographic high. Both sets of hysteresis experiments show lock-in behavior.

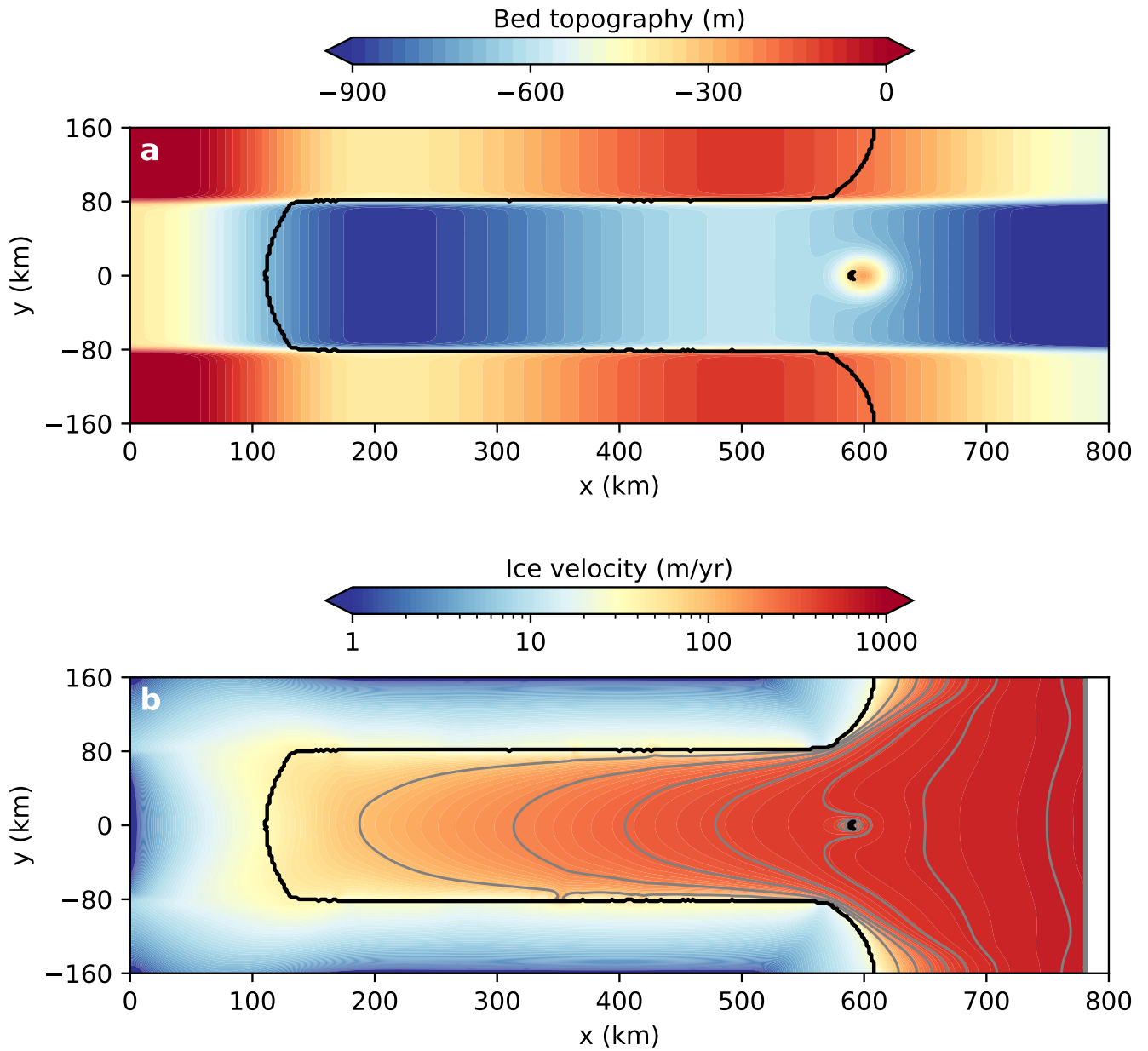


Figure S6. (a) Channel-type bed topography prescribed in the laterally confined simulations for the case of a deep bed depression ($D_{BD} = 900$ m) with a topographic high at a depth of $D_{TH} = 260$ km, located at $x_{TH} = 600$ km. The steady-state grounding-line position of the re-grounded ice-sheet-shelf system and its pinning point are shown by the black contours. (b) Surface speed of the laterally confined ice-sheet-shelf system on a logarithmic scale with speed contours of 100 m/yr spacing in grey.

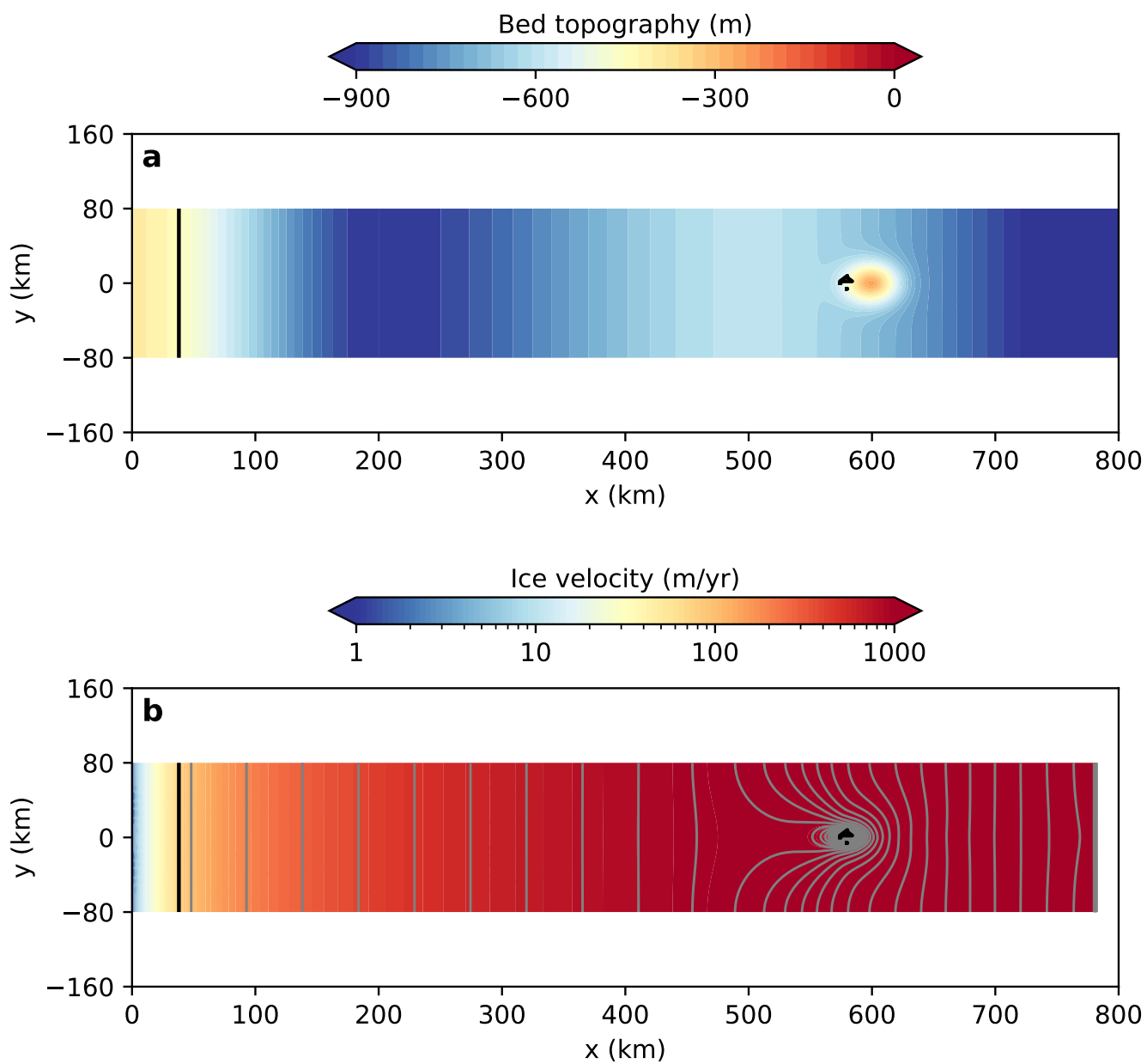


Figure S7. Same as Fig. S6 but here for the laterally unconfined version.